

STUDY OF THE FEASIBILITY OF ACOUSTIC LINERS INSIDE THE BEAM THAT INTERACTS WITH A UAV DRONE ROTOR

Santiago Montoya-Ospina[1], Romain Gojon[1], Hélène Parisot-Dupuis[1], Frank Simon[2]

[1]ISAE-SUPAERO, 10 Avenue Marc Pélegrin, Toulouse, 31055, France
[2]DMPE - ONERA - Université de Toulouse, F-31055, Toulouse, France

Abstract

This paper addresses the growing demand for advancements in rotorcraft technology by proposing the concept of acoustic liners integrated within surfaces surrounding a rotor with the main objective of noise mitigation. The study is involving a rotor working in installed conditions, where a beam simulates the connection between the propulsion system and the airframe of a classical drone configuration. The primary objective is to evaluate experimentally the feasibility of an integrated liner as passive noise reduction strategy and to assess its impact on the aerodynamic performance of rotors. The concept proved to be effective in reducing noise at the harmonics of the BPF, which is particularly important in installed conditions.The prototype design based on a Long Elastic Open Neck Acoustic Resonator (LEONAR), together with the associated experimental methodology, aim to contribute to the field of rotor aeroacoustics and support the development of innovative technologies for mitigating rotorcraft noise.

Keywords: Drone, rotor, liner, resonator, prototype

1. Introduction

This paper addresses the growing demand for advancements in rotorcraft technology by proposing the concept of acoustic liners integrated within surfaces surrounding a rotor with the main objective of noise mitigation.

More precisely, a rotor in installed conditions is investigated, with a beam used to represent the connection between the propulsion system and the airframe of a conventional drone or VTOL configuration (Figure 1).



(a) (b)

Figure 1 - Examples of VTOL drones. (a) Meituan's delivery drone taken from MIT Technology review, (b) EHang 184 taxi drone taken from Flexbot - Accessed on 01-02-2025.

The main objective of the present paper is to evaluate experimentally the feasibility of an integrated liner as passive noise reduction strategy. The liner is integrated within the structure of the beam.

A secondary objective is to assess the impact of the liner on the performance of the propulsive system.

The main acoustic sources of a rotor in interaction with a beam are presented In Figure 2. This simplified test case provides a good benchmark application for the proposed integrated liner.

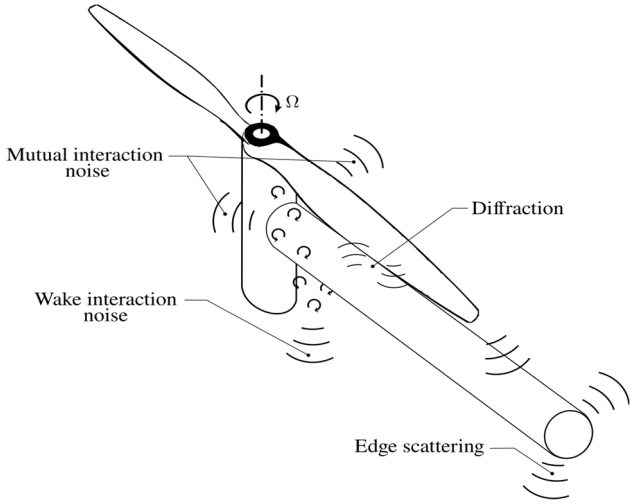


Figure 2 - Schematic of the different types of noise sources emerging from the interaction of the blades of a rotor and a beam (excluding the thickness noise of the rotor).

Several teams have worked on installed rotors recently. Depending on the setup considered, potential interaction noise or scattering effects were the main contributors to the acoustic spectrum at harmonics of the Blade Passing Frequency (BPF):

1.1 Potential Interaction Noise

This mechanism arises from the interaction between the potential fields of the rotor blades and nearby surfaces (e.g., beams or struts), leading to unsteady aerodynamic loading on both the blades and the beam [1].

Wu et al. [2] and Roger et al. [3] have addressed this mechanism considering the effect of mutual potential interaction between the rotor blades and a beam and their effect on the steady and unsteady loading on each component.

Two 2-D unwrapped uncoupled models relying on the potential flow theory around a cylinder are derived for the unsteady loadings on the rotor and the beam at every radial location [4].

1.2 Diffraction

The sound waves produced by the rotor can be diffracted by the beam, and conversely, the sound waves from the beam can also be diffracted by the rotor blades. Evanescent acoustic waves for isolated rotor may become significant in the far field due to their diffraction by either the beam or the rotor blades.

Diffraction becomes important when the size of the body is larger than the size of the rotor. In a study by Cros et al. [5], which simulated a marine propeller under installed conditions, it was found that the scattered pressure field is comparable in magnitude to the incident pressure field.

Please note that, in this setup, the rotation axis and the beam axis are parallel, in contrast with the setup discussed above. Additionally, the distance from the source to the surface, relative to the characteristic attenuation distance of evanescent waves from the sources, is a crucial parameter.

When the sound from the rotor impinges on an edge, like a beam tip, it is scattered and can lead to amplified sound in certain directions. This is important in configurations where the rotor blades pass close to structural edges, causing scattered noise to affect the acoustic signature in the far-field. The

effect is more pronounced at higher harmonics of the BPF, and the directivity pattern of the scattered sound often changes based on the geometry and proximity of the structure. Edge scattering is modeled using tailored Green's functions and diffraction theories, which predict how noise behaves when interacting with surfaces.

The starting point of the present study is an existing academic configuration that has been investigated through experimental [1], analytical [4], and numerical [6] methods.
A two bladed constant pitch and constant cord 20 cm diameter rotor interacts with a cylindrical beam that has a diameter of 20 mm. The center of the beam is positioned 20mm below the rotor disk plane. Gojon et al. [1] tested this assembly in an anechoic room and found that the presence of the beam did not affect the Sound Pressure Level (SPL) at the BPF compared to the case of the isolated rotor. However, the farfield acoustic radiation of the two surfaces assumed to be the main acoustic sources, namely the rotor and the beam, presented on Figure 3, at a rotational speed of 8000 RPM, show that the presence of the beam significantly impacted the BPF harmonics, where the levels were notably higher [7].
The Figure 4 shows SPL amplitudes for a microphone positioned on the rotor-disk plane, from BPF and harmonics, generated by the unsteady loading on the beam surface [6].
Doué et al. used the Ffowcs Williams & Hawkings (FW-H) analogy formulation to evaluate 13 axial slice contributions to the far-field sound pressure. The figure displays the amplitudes for the BPF and its harmonics, illustrating the source amplitudes along the beam span as a fraction of the rotor tip radius. It is important to note that this approach ignores interactions between the slices. The figure indicates that sources from 3BPF to 9BPF produce notable sound levels, with 5BPF being the most pronounced across most of the beam span. Therefore, we concentrated on 5BPF when designing the liner to integrate within the beam structure.

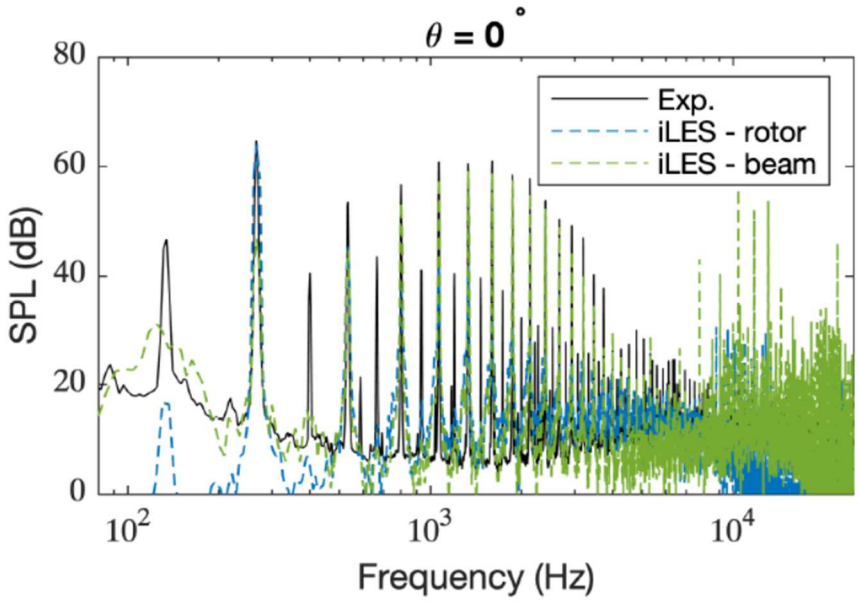


Figure 3 – Ex. of simulated farfield acoustic radiation (dB) of the rotor and beam surfaces – comparison with experimentation– issued from [7].

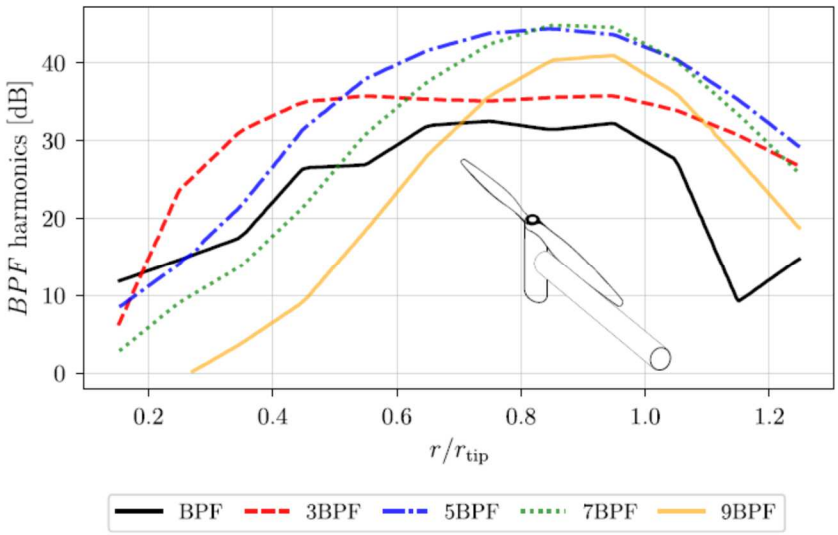


Figure 4 – Ex. of SPL (dB) of the BPF harmonics generated by the sources located on the beam surface interacting with the rotor – issued from [6].

2. Design of a Lined Beam that Interacts with a Small-Scale Rotor

The liner to integrate into the beam is based on a SDOF LEONAR configuration [8,9].

Figure 5 shows a schematic of an SDOF LEONAR configuration formed by a perforated plate facesheet, backed by a cavity with walls that are rigid and connected by elastic tubes from the plate holes to the cavity. Such a simple configuration could be designed to target a single frequency. Nevertheless, multiple configurations can be achieved to target a broader frequency range such as 2DOF configurations by stacking two SDOF arrays one over the other, including multiple partitions inside the cavity where the tube lengths are different, etc. This type of liner allows having cavity lengths lower than $\lambda/30$ while absorbing noise at low frequencies.

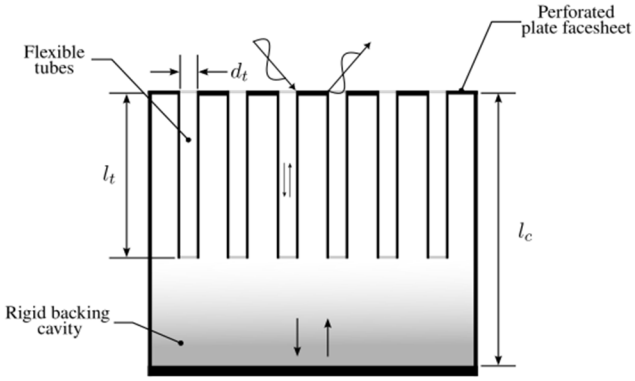


Figure 5 - Schematic of a SDOF LEONAR liner configuration defined by a perforated plate facesheet with porosity σ_{fs}, (hole surface / liner surface) backed by a rigid cavity of length l_c, and linked by flexible tubes of length l_t and diameter d_t.

In the case of integration into the beam, the principle is to insert hollow tubes inside internal resonating cavities which span the whole circumference. Only half the circumference of the cylinder facing the rotor is treated. The cavity volume is divided into 24 cavities (Figures 5 and 6) along the beam axis and 4 hollow tubes per cavity (internal radius 1 mm, length 4 mm), providing a resonance frequency of 1334 Hz, corresponding to 5BPF.

The Figure 9 illustrates the absorption coefficient, which is at its maximum at the resonance frequency, for the liner configuration obtained by FEM simulations conducted in COMSOL Multiphysics® v. 5.6 (Figure 8).

In practice, the simulations use the thermoviscous acoustics module in the frequency domain, which employs the linearized Navier-Stokes equations. The primary objective of these simulations are to determine the resulting absorption coefficient (and the acoustic impedance) for a specific frequency

range. The setup simulates an impedance tube scenario, where plane waves excite a sample of the liner. We measured the acoustic variables, including sound pressure and particle velocity, along a surface defined within the impedance tube to calculate the acoustic impedance and absorption coefficient.

We can see that maximum absorption occurs near the target frequency of the 5BPF, in spite of the limited cavity thickness.

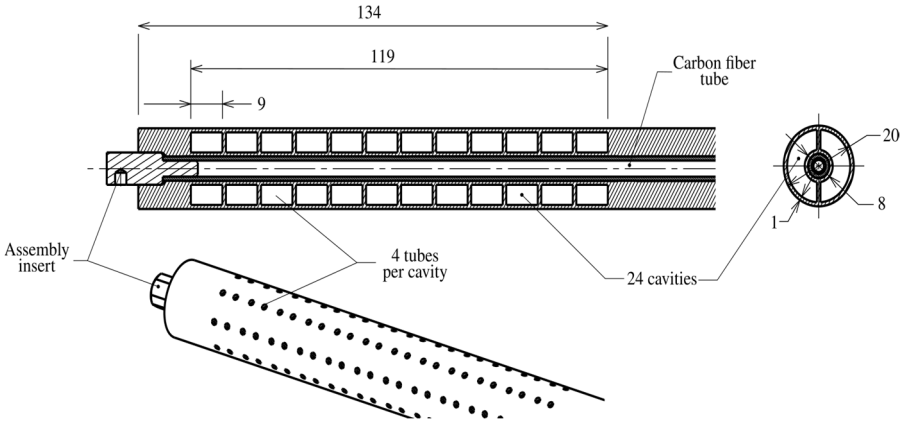
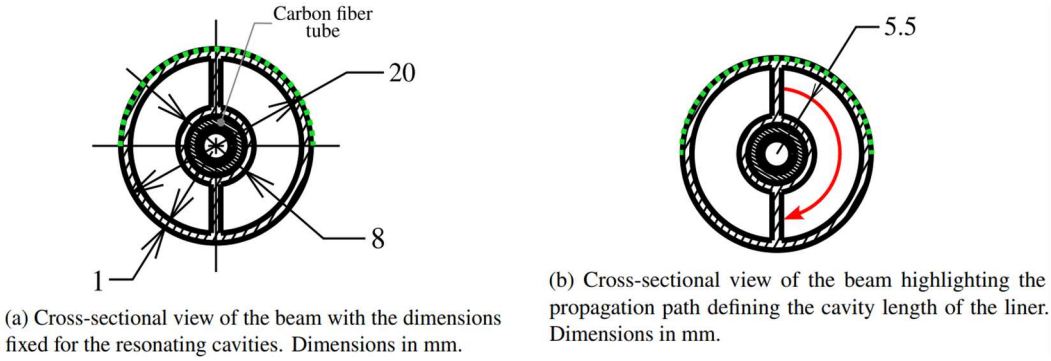


Figure 6 - Snapshot of the CAD model assembly of the beam that will integrate the liner designed to have maximum absorption at 5BPF. The tubes are inserted inside the two internal cavities which span the whole circumference, however the lined surface corresponds to half circumference. Dimensions in mm.



(a) Cross-sectional view of the beam with the dimensions fixed for the resonating cavities. Dimensions in mm.

(b) Cross-sectional view of the beam highlighting the propagation path defining the cavity length of the liner. Dimensions in mm.

Figure 7 - Schematic of the cross-sectional views of the beam depicting the resonating cavities. Dimensions in mm. The green dotted lines show the area to be lined.

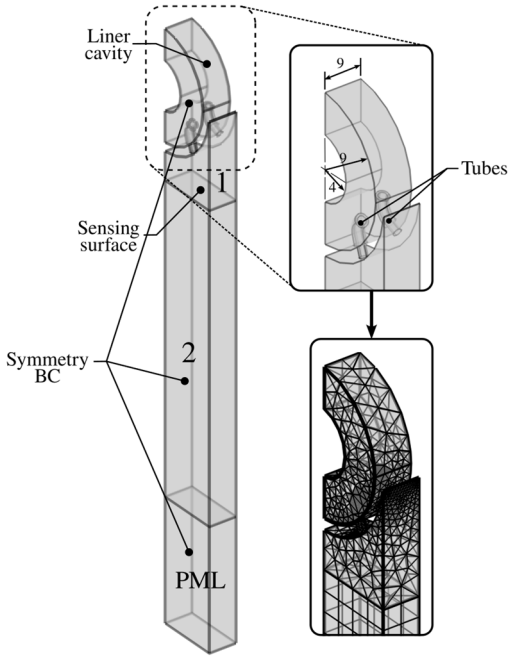


Figure 8 - COMSOL geometry setup of the liner configuration to be inside the beam designed to have maximum absorption at 5BPF.

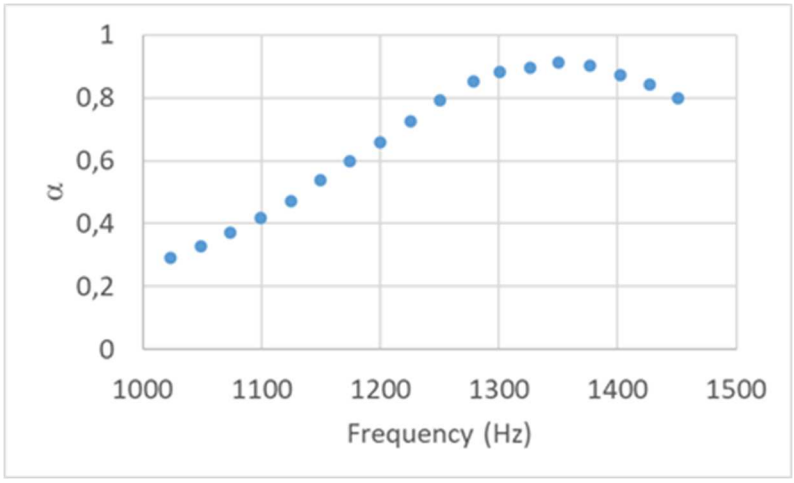
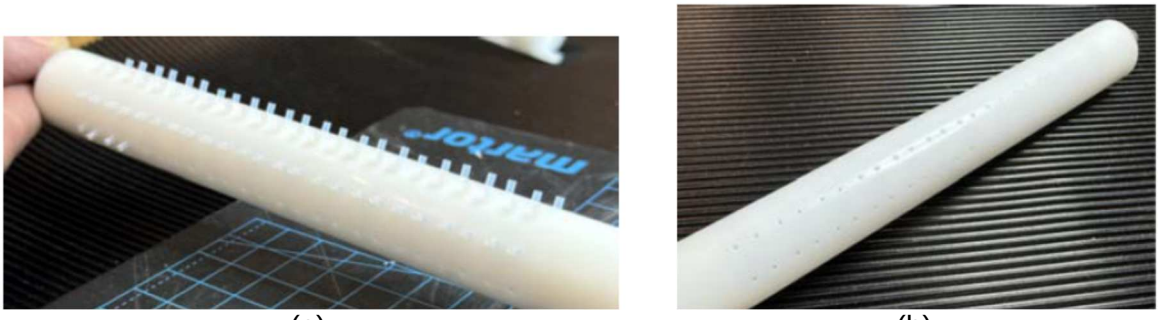


Figure 9 – Absorption coefficient of the liner configuration to be integrated inside the beam designed to have maximum absorption at 5BPF obtained with FEM method.

The Figure 10 shows the liner prototype manufactured using SLA 3D printing. The beam was sand and polished providing smooth surfaces. The tubes were cut with the length and preassembled in the beam holes. Finally, the tubes were inserted into the cavities up to the beam surface forming the liner structure.



(a) (b)

Figure 10 – Preassembly of the tubes in the holes (a) and full assembly of the beam (b).

3. Aerodynamics and Acoustic Measurements

The experimental setup (Figure 11) allows us to measure aerodynamic and acoustic variables simultaneously. This setup is located inside the anechoic room at ISAE-SUPAERO, which is dedicated to investigating the aeroacoustics of low Reynolds number rotors.

3.1 Aerodynamics

Aerodynamic loads are measured with an ATI Nano17 load cell coupled directly beneath the motor.

Let us begin by comparing the loading coefficients of the rotor in interaction with the Rigid beam or the Lined beam at 8000 RPM. It appears a minor drop in the Thrust coefficient (6.15 vs 6.25) and no significant impact on the Torque coefficient (3.9 vs 4).



Figure 11 – Rotor noise test bench inside the anechoic room of ISAE-SUPAERO.

3.2 Acoustic measurement

Regarding acoustics, an antenna using 13 GRAS 40PH-10 microphones constitutes an arc array of 1.62 m of radius measured from the center of the rotor.

Experimental 3D directivities are shown at a specific frequency (5BPF for instance). The Figure 12 compare the rotor directivity interacting with the rigid beam, represented as a transparent gray surface superposed with the directivity of the rotor interacting with the lined beam, illustrated as a colored surface for each frequency of interest. In addition, a schematic of the rotor-disk plane and the beam are included to facilitate the analysis of the results.

At BPF, we clearly see a well-defined vertical dipole, where the levels approach a minimum along the rotor axis, indicating the dominance of steady loading noise at this frequency.

For the other frequencies, the pattern shifted to a “horizontal” dipole-type with minima along the beam axis, indicating the dominance of unsteady loading noise from the beam. These results align with those obtained by Gojon et al. [1] experimentally, and by Vella et al. [4], both analytically and numerically.

Regarding the effect of the liner, no significant impact was observed at BPF. At the other frequencies, a clear reduction in levels is observed, particularly in the upper hemisphere (above the rotor-disk plane). Conversely, the lined beam increased noise in the lower hemisphere (below the rotor-disk plane) at azimuthal angles around the beam axis, especially noticeable at 5BPF. We may attribute this effect to the liner presence only on the upper half circumference of the beam. We achieved noise reduction at the target frequency (5BPF) and influenced other frequencies surrounding

this target frequency.

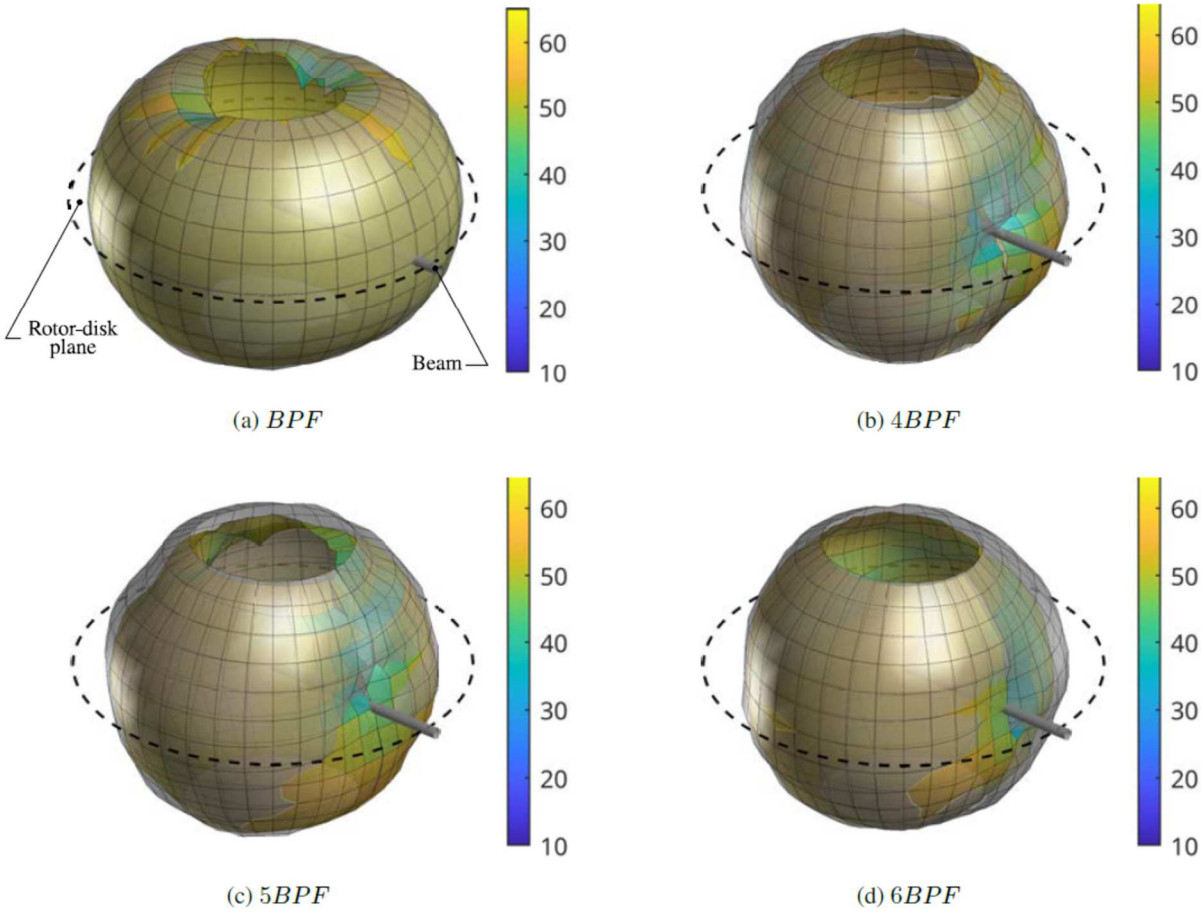


Figure 12 – Experimental 3D SPL directivity of the two-blades rotor interacting with the rigid beam (light gray surface) and the lined beam (colored surface) designed to have maximum absorption at 5BPF.

The sound power, *W*, can be written as the acoustic intensity, *I*, passing through a defined surface, *S*:

$$W = \iint_S I dS \tag{1}$$

If we assume that our measurements are performed in the far-field, so we can assume that only plane waves arrive to the microphones, we can approximate the normal component of the acoustic intensity in terms of the sound pressure and the impedance of the medium. It is important to note that this approximation can be debated at lower frequencies (for the BPF harmonics for instance); nevertheless, we will use it to assess the overall effectiveness of the treated beams. Additionally, as the location of the microphones in our antenna describes a spherical shell surface, we can approximate (1) as:

$$W = \int_0^{2\pi} \int_{\frac{\pi}{6}}^{\frac{5\pi}{6}} \frac{p_{rms}^2}{\rho_0 c_0} r_{ant} sin\theta d\theta \varphi \tag{2}$$

with r_{ant} the radius of the microphone antenna which is equal to 1.62 m, and the integration limits of the elevation angles correspond to the experimental setup in Figure 11.

The resulting sound power will be partial, since the antenna did not cover an entire sphere in the experimental setup.

For the calculation of the attenuation of the first 20 harmonics of the BPF, the value of p^2_{rms} was taken as the root mean square value in the autospectra of each microphone of the antenna at each elevation and azimuthal position. Then, using (2), the sound power was calculated for each BPF harmonic.

The same was done for the overall sound power, but instead the value of p^2_{rms} was obtained by integrating the autospectrum of each microphone between 80 and 16000 Hz for each elevation and azimuthal angle.

Finally, the SWL (Sound Power Level) for each harmonic was calculated as:

$$SWL(f) = 10log_{10}\left(\frac{W(f)}{W_{ref}}\right) \quad \text{with } W_{ref} = 10^{-12}W \tag{3}$$

The attenuation can be finally calculated as the difference in levels between the rigid and lined beam for the BPF harmonics: $\Delta SWL(f) = SWL_{rigid}(f) - SWL_{liner}(f)$.

The Figure 13 illustrates the SWL (dB) amplitudes provided by the rigid and the lined beams for the 20 first BPF harmonics. While Figure 14 illustrates the attenuation provided by the treated beam for each of these harmonics.

It appears that the lined beam provides an attenuation on a large frequency range, i.e. from the 6BPF to the 14BPF, with maxima at 8BPF and 11BPF. This phenomenon may be attributed to the absorption characteristics associated with the resonant effect of the liner, as a distinct effect became apparent from 5BPF onward.

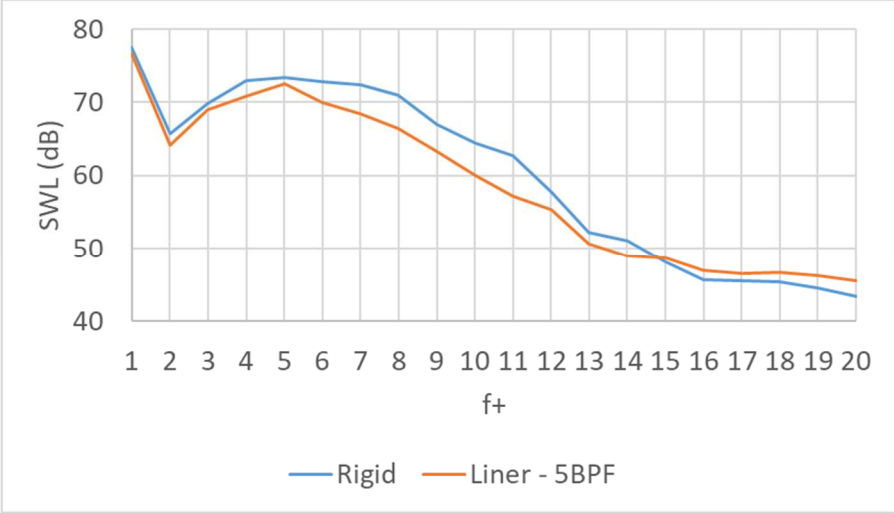


Figure 13 – SWL (dB) amplitudes of the first 20 harmonics of the BPF for the rigid and liner beams. The BPF harmonics are shown in terms of the reduced frequency, f+ = f/BPF.

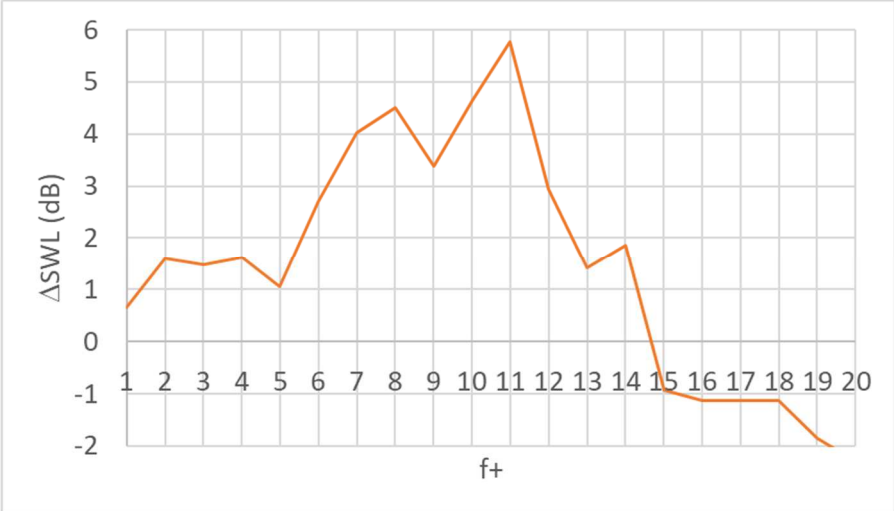


Figure 14 - SWL attenuation (dB) of the first 20 harmonics of the BPF. The BPF harmonics are shown in terms of the reduced frequency, f+ = f/BPF.

4. Conclusion

In this paper, the integration of a thin liner based on LEONAR concept [8,9] is proposed in a beam interacting with a two bladed rotor. The liner has been designed to target BPF harmonics arising from the rotor installed condition. The experimental results demonstrate that such liner permits to reduce noise at BPF harmonics, with reductions up to 5 dB observed.

The idea of integrating acoustic liners within beams could also be applied to various aircraft types. For example, innovative designs for electric or hybrid planes that use wing-mounted engines with distributed propulsion systems might gain advantages from this concept. Research indicates that such aircraft can produce higher levels of unsteady loading noise [10], which could be mitigated by using acoustic liners within in the wings. Furthermore, the constraints related to space and size within an aircraft wing could be reduced, making it easier to design and install the liners.

5. Contact Author Email Address

Mail to: frank.simon@onera.fr

6. Copyright Statement

The authors confirm that they, and/or their company or organization, hold copyright on all of the original material included in this paper. The authors also confirm that they have obtained permission, from the copyright holder of any third party material included in this paper, to publish it as part of their paper. The authors confirm that they give permission, or have obtained permission from the copyright holder of this paper, for the publication and distribution of this paper as part of the ICAS proceedings or as individual off-prints from the proceedings.

References

[1] Gojon R, Parisot-Dupuis H, Mellot B, and Jardin T. Aeroacoustic radiation of low Reynolds number rotors in interaction with beams. *The Journal of the Acoustical Society of America*, Vol. 154, No. 2, pp. 1248–1260, 2023. doi: 10.1121/10.0020672.

[2] Wu Y, Kingan M.J and Go S.T. Propeller–strut interaction tone noise. *Physics of Fluids*, vol. 34, no. 5, p. 055 116, 2022. doi: 10.1063/5.0090187.

[3] Roger M, Vella E, Rendon J, and Moreau S. Aerodynamic and Sound-Scattering Effects in Rotor-Strut Interaction Noise of Small-Size Drones, *AIAA AVIATION 2023 Forum*, American Institute of Aeronautics and Astronautics, 2023. doi: 10.2514/6.2023-4523.

[4] Vella, E., Gojon, R., Parisot-Dupuis, H., Doué, N., Jardin, T., & Roger, M. Mutual Interaction Noise in Rotor–Beam Configuration. *AIAA Journa*l, 1-16, 2026.

[5] Cros E, Roger M, and Serre G. Low-frequency amplification of propeller tonal noise due to the scattering by a compact rigid cylinder, *Journal of Sound and Vibration*, vol. 546, p. 117 450, 2023. doi: 10.1016/j.jsv.2022.117450.

[6] Doué N, Gojon R, and Jardin T. Numerical Investigation of the Acoustics Radiation of a Two-Bladed Rotor in Interaction with a Beam. *Fluid-Structure-Sound Interactions and Control, Kim D, Kim K C, Zhou Y, and Huang L,* Eds., Singapore: Springer Nature, pp. 169–176, 2024. doi: 10.1007/978-981-97-6211-8_23.

[7] Gojon R, Doué R, Parisot-Dupuis H, Mellot B, and Jardin T. Aeroacoustic radiation of a low Reynolds number two-bladed rotor in interaction with a cylindrical beam. *28th AIAA/CEAS Aeroacoustics 2022 Conference,* American Institute of Aeronautics and Astronautics, 2022. Doi: 10.2514/6.2022-2972.

[8] Simon F. Long Elastic Open Neck Acoustic Resonator for low frequency absorption. *Journal of Sound and Vibration*, Vol. 421, pp. 1–16, 2018. doi: 10.1016/j.jsv.2018.01.044.

[9] Simon F. Garniture Surfacique pour Absorption Acoustique. INPI Patent n°3.065.570, May, 3 2019.

[10] Acevedo Giraldo D, Roger M, Jacob M. C. and Beriot H. Analytical study of the aerodynamic noise emitted by distributed electric propulsion systems, *28th AIAA/CEAS Aeroacoustics 2022 Conference*, American Institute of Aeronautics and Astronautics, 2022. doi: 10.2514/6.2022-2830.